Eur. Phys. J. D **42**, 393–396 (2007)
DOI: 10.1140/epjd/e2007-00046-4

THE EUROPEAN PHYSICAL JOURNAL D

Kinetic energy release for the collision-induced dissociation of CO^+

G. García[1,2], E. Mejía-Ospino[1,2,a], A. Guerrero[1], I. Álvarez[1], and C. Cisneros[1]

[1] Centro de Ciencias Físicas, Universidad Nacional Autónoma de México, Cuernavaca, Mor. Apdo. Post. 48-3, C.P. 62210, México, Mexico
[2] Laboratorio de Espectroscopía Atómica y Molecular, Universidad Industrial de Santander, Bucaramanga A.A.678., Colombia

Received 27 November 2006 / Received in final form 12 January 2007
Published online 2nd March 2007 –

Abstract. The kinetic energy release distributions (KERDs) of C^+ and O^+ fragments arising from 5 keV collision-induced dissociation (CID) of CO^+ ions with helium have been measured. The KERDs of C^+ and O^+ exhibit different features corresponding to the states that participate in CID processes. We have identified groups of dissociative and predissociative states, and compare them with theoretical and experimental values.

PACS. 34.20.Mq Potential energy surfaces for collisions – 34.50.-s Scattering of atoms and molecules – 34.50.Gb Electronic excitation and ionization of molecules; intermediate molecular states (including lifetimes, state mixing, etc.)

1 Introduction

Carbon monoxide is the second most abundant molecule in the Universe after molecular hydrogen, and is present in a wide variety of astrophysical environments. Therefore, it is very important to investigate the CO^+ ion to obtain information on the physical and chemical processes taking place in the atmospheres of planets. Singly charged carbon monoxide has been observed less often in such environments [1]. Studies on the CID of the CO^+ ion are scarce. However, studies on the photoionization as well as the dissociative recombination and excitation of CO^+ ion are abundant [2–8].

In any collisional interaction between ions and neutral molecules, the perturbation caused to the projectile ion by the neutral target molecule leads to collisional excitation of the former. If the vertical excitation energy is much larger than the dissociation energy of the projectile ions, then the projectile ion could undergo fragmentation. CID can be used to study several different fundamental properties. CID technique has been widely used for the determination of structure and fragment pathway analysis, as well as to obtain fundamental information about the electronic structure of the projectile and of the dissociation products [1,9–15]. The first work about the collision of CO^+ with molecules appeared in 1957, when Melton and Wells [16] studied the CID of CO^+ with H_2, D_2, N_2 and CO. They measured the relative cross sections for dissociation of CO^+ with respect to dissociation with He using projectile energies of 1 to 5 keV. The cross sections for the CID of CO^+ with H_2, N_2 and SF_6 have previously been reported by our laboratory [17].

With regard to the electronic structure, Dowek et al. [13] studied the He^+–CO and He–CO collisions to find the different electronic states of CO and CO^+. Their results show a Rydberg series from 11 to 14 eV for the CO. They could also identify the excited states $A^2\Pi$, $B^2\Sigma^+$, $C^2\Sigma^+$, $D^2\Pi$ and $F^2\Sigma^+$ of CO^+. Krishnamurthi et al. [18] used the CO^+–H_2 collision to study excitation to states $B^2\Sigma^+$, $C^2\Sigma^+$ and $D^2\Pi$, with projectile energies of 1.8 keV. Dentamaro and Katayama [19] studied the transition between the $A^2\Pi(v=0)$ and $B^2\Sigma^+(v=0)$ states of CO^+ using CID. Moran et al. [20] measured the threshold of dissociation of CO into C^+ and O using CID from 0.65 to 3.2 keV, and their results show a threshold of dissociation at 19.5 ± 1.0 eV. Lu, Tosi and Bassi [12] studied the $CO^+ + CO$ reaction and found the appearance potential of C^+ at 2.5 ± 0.1 eV. The KERDs for dissociative ionization and dissociative excitation of CO^+ into C^+ and O^+ fragments have recently been reported using crossed electron-ion beam experiments [21]. In this work, it was possible to separate the two dissociation processes and identify some states that contribute to the dissociation of CO^+. Theoretical studies to calculate the potential energy surfaces of the ground and excited electronic states of CO and its singly charged ion have been carried out by many researchers with varying degrees of success [22–28]. We wish to give emphasis to the work of Honjou and Sasaki [23], because their calculations allow us to interpret our results regarding kinetic energy release (KER).

[a] e-mail: emejia@uis.edu.co

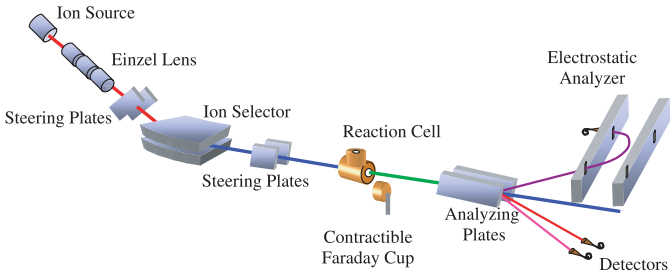

Fig. 1. Schematic experimental apparatus.

In this work, we have measured the KERD in the laboratory frame, of C^+ and O^+ fragments arising from the CID of CO^+ ions with helium at 5 keV.

2 Experimental

The present apparatus is practically the same as that used previously [17,29,30]. A schematic diagram of the experimental apparatus is shown in Figure 1. The CO^+ beam was electrostatically accelerated at 5 keV ($E_0 = 5$ keV), its momentum was analyzed by means of a magnetic mass spectrometer, and it was passed through a series of collimators before entering the gas cell. The beam interacted with the gas in the cell and the CO^+ dissociated to either C^+ and O or C and O^+. The dissociation products entered the detection chamber and were mass/charge separated by an electric field produced by applying an appropriate voltage to a pair of plates. This field diverted the charged fragments 12° from the path of the undeflected beam. On one side, a parallel-plate electrostatic analyzer was located 20 cm away from the edge of the plates and oriented at 45° between the charged fragment direction and the field. A channel electron multiplier (CEM) was positioned at the exit of the analyzer. A rectangular slit of 0.3 mm width and 10 mm length was placed in front of the CEM, and a collimator of 2.8 mm diameter located at the entrance of the energy analyzer provided the energy analysis of the charged fragments by sweeping the applied voltage between the plates of the analyzer. These conditions result in an energy resolution ($\Delta E/E$) of 0.04. In this work, the parallel-plate analyzer was used to record the energy distribution of the C^+ and O^+ fragments. On the opposite side from the undeflected beam, a CEM with a 0.9-cm-diameter active area was located in order to record the total fragment count rate. A retractable Faraday cup was placed at the exit of the target cell to measure the total current of the diatomic beam. The detectors and the analyzer were shielded to prevent unwanted readings. This setup allows the measurement of the laboratory energy distribution of the charged fragments as well as the current intensity of the initial ion beam, and the total intensity of the fragments, which are necessary for a determination of the absolute total cross sections. However, in this work, we have not measured the cross section.

3 Results and discussion

The main dissociation paths of CO^+ lead to the production of ionic fragments C^+ or O^+ through the reactions

$$CO^+ + He \rightarrow C^+ + O^0 + He \quad (1)$$

$$\rightarrow C^0 + O^+ + He \quad (2)$$

and

$$\rightarrow C^+ + O^+ + He + e^-. \quad (3)$$

If we consider the decomposition of CO^+ with mass m_{CO+} and kinetic energy $E_0 = 5$ keV, the elastically and inelastically scattered CO^+ ions appear at kinetic energies around 5 keV. The C^+ and O^+ fragments appear at energies centered around $E_{C^+} = (m_{C^+}/m_{CO^+})E_0$ and $E_{O^+} = (m_{O^+}/m_{CO^+})E_0$. During the collision, part of the kinetic energy of the CO^+ ion is transformed into internal excitation energy of the projectile, yielding CO^{+*} in dissociative or metastable states lying at different energies W above the $C^+ + O$ or $C + O^+$ dissociative limits. The reaction can be written as a two-step mechanism [31,32]:

$$CO^+(E_0, \alpha_0, E_I) + He \rightarrow CO^{+*}(E_0 - E^{*\prime}, W, \theta) + He$$

$$\rightarrow C^+(E_{C+}, \alpha) + O \quad (4)$$

$$\rightarrow C + O^+(E_{O+}, \beta) \quad (5)$$

where E_0 is the kinetic energy of the primary CO^+ beam, α_0 is the angle between the internuclear axis and the flight direction of the CO^+ ions, E_I is the initial internal energy of CO^+, E_{C+} and E_{O+} are the C^+ and O^+ laboratory kinetic energies, α and β are the angles between the CO^+ flight direction and the C^+ and O^+ directions, and $E^{*\prime}$ is the total projectile-kinetic-energy loss. W, the excess internal energy of CO^{+*} above the dissociation limit, is transformed into center-of-mass (c.m.) translational energy of the fragments. In this two-step mechanism, θ is the angle between the flight direction of the transient CO^{+*} and the initial flight direction. In scattering experiments involving keV energy collision and light target, this angle is generally assumed to be negligible.

Measurement of the fragment laboratory KERD allows us to determine the energies W of the predissociative or dissociative states reached during the collision with respect to their associated dissociation limit, and therefore gives information on the mechanism of dissociation. Because of the accurate angular discrimination of the parent and fragment ions (C^+ or O^+), the excess energy W released in the c.m. is associated with either forward (+) or backward (−) motion of charged fragments having discrete and well-defined kinetic energies in the laboratory frame:

$$E^{\pm}_{C^+} = \frac{m_{C^+}}{m_{CO^+}}(E_0 - E^{*\prime}) \pm \frac{2}{m_{CO^+}}\sqrt{m_{C^+} m_O [W(E_0 - E^{*\prime})]} + \frac{m_O}{m_{CO^+}} W \quad (6)$$

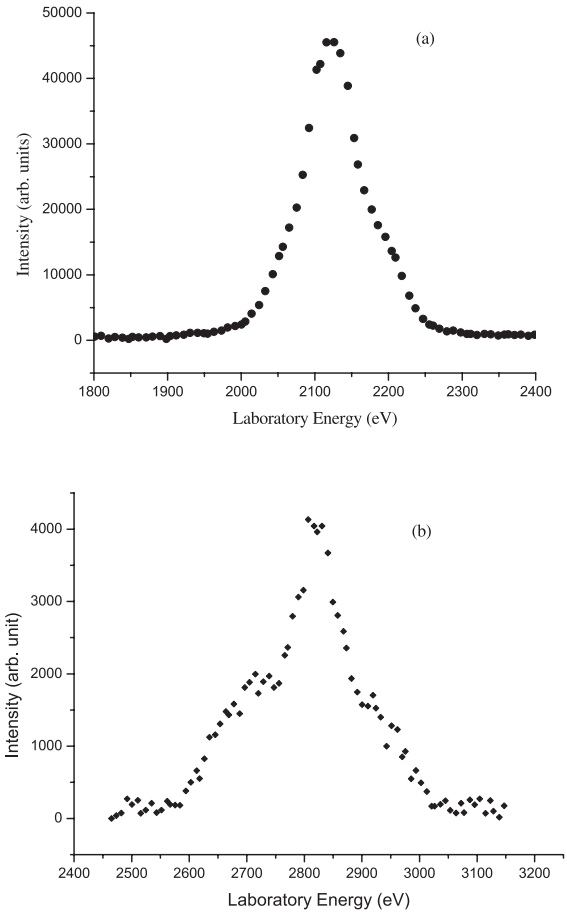

Fig. 2. Typical translational energy spectrum observed in the laboratory frame for (a) C^+ and (b) O^+ CID product ions in CO^+ + He experiments at 5 keV.

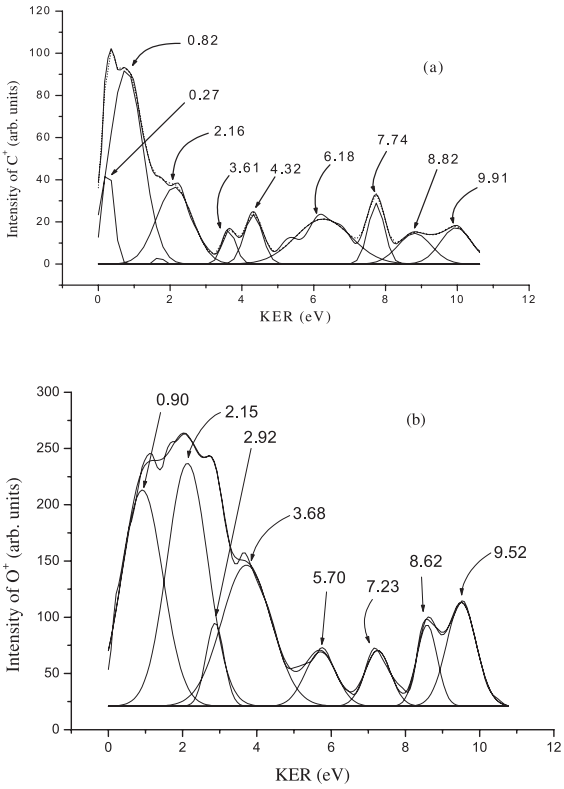

Fig. 3. Typical kinetic energy release distributions observed in the centre-of-mass frame for (a) C^+ and (b) O^+ CID product ions in CO^+ + He experiments at 5 keV.

or

$$E^{\pm}_{O^+} = \frac{m_{O^+}}{m_{CO^+}}\left(E_0 - E^{*\prime}\right) \pm \frac{2}{m_{CO^+}}\sqrt{m_{O^+}m_C\left[W(E_0 - E^{*\prime})\right]} + \frac{m_C}{m_{CO^+}}W. \quad (7)$$

The experimental measurement of W and $E^{*\prime}$ allows the determination of the energies of the dissociative states reached during the collision, provided that the initial states of the parent ion are known [31–34].

The translational-energy spectrum of the C^+ and O^+ fragments produced when a 5 eV CO^+ beam collides with a helium-gas target are shown in Figures 2a and 2b. These spectra have been recorded by scanning the voltage applied across a calibrated electrostatic energy analyzer. Careful inspection of Figures 2a and 2b show that the maximum of both energy distributions are slightly shifted to the left of the position that corresponds to zero energy loss, $E_{C^+} = 2142.86$ and $E_{O^+} = 2857.14$. This shift in the peak position arises from the loss of energy during the collision, which in turn is a measure of the increment in internal energy of the molecule. In the translational-energy spectra, it is possible to observe several shoulders on both sides of the central peak; these shoulders corresponding to the excess energy released in either forward or backward motion of the charged fragments in the laboratory frame.

In order to clarify this matter, the KERD in the centre-of-mass frame for dissociation into C^+ + O and C + O^+ was obtained (Figs. 3a and 3b). We have assumed an isotropic angular distribution of the ejected fragments. The structures shown in the spectra correspond to KER at collision energy of 5 keV. The spectra are presented with a Gaussian fit, and it is possible to observe the KER values corresponding to the initial and final states in the dissociation process. We assume that each peak correspond to the KER when the molecular CO^+ ion dissociates through a C^+ + O, C + O^+ or C^+ + O^+ channel. Table 1 presents the observed KER for reactions (1), (2) and (3). For comparison, we have also presented other experimental and theoretical reports [1,22–26]. The agreement between the experimentally measured KER distribution and the components deduced from the theoretical calculation is good.

We can see in Figures 3a and 3b the presence of fragments with KER as large as 9.91 eV (total KER $\sim$ 23.12 eV), and it is clear that highly excited states ($E^2\Sigma^+$, $E'^2\Sigma^+$ and $^2\Pi_{VI}$) are involved in the dissociation process. In addition, these highly excited states of CO^+ can populate some CO^{2+} states. We assume that CO^{2+} dissociates spontaneously into C^+ + O^+ through $^3\Sigma^+$, $^1\Sigma^-$, $^1\Sigma^+_{III}$ and $^1\Sigma^+_{IV}$.

Table 1. Comparison of the present experimental results for the KER against previous theoretical studies.

Process	Final state	Theoretical results[a]	Present results[b]	
		KER (eV)	Fragment KER(eV)	KER (eV)
$CO^+ + He \rightarrow C^+ + O^0 + He$	$^4\Delta$, D $^2\Pi$	0.6	0.27	0.63
	$^4\Pi$, $^2\Sigma^-_{\rm I}$	2.0	0.81	1.89
	E $^2\Sigma$, $^2\Pi_{\rm IV}$,$^2\Pi_{\rm V}$	4.3	2.03	4.74
	3 $^2\Pi$	6.4	2.86	6.74
	E $^2\Sigma^+$, E$'$ $^2\Sigma^+$	7.5	3.61	8.42
$CO^+ + He \rightarrow C^0 + O^+ + He$	$^6\Sigma^+_{\rm I}$	2.5	0.90	1.58
	$^4\Sigma^+_{\rm II}$	4.1	2.15	3.76
	$^2\Sigma^+_{\rm VI}$	4.9	2.92	5.11
	$^2\Pi_{\rm VI}$	6.0	3.68	6.44
$CO^+ + He \rightarrow C^+ + O^+ + He$	$^3\Sigma^+$	9.4	4.07(5.70)	9.50(9.98)
	$^1\Sigma^-$	11.8	6.18(7.23)	14.42(12.65)
	Not assigned	-	7.00(8.62)	16.33(15.09)
	$^1\Sigma^+_{\rm III}$	17.6	7.74(9.52)	18.06(16.66)
	$^1\Sigma^+_{\rm IV}$	19.1	8.82	20.58
	Not assigned	-	9.09	21.21
	Not assigned	-	9.91	23.12

[a]References [1,22–26], [b]values in parentheses correspond to the KER observed in the KERD of the O^+ fragment.

4 Conclusion

KERDs for C^+ and O^+ fragments arising from the CID of CO^+ ions with helium have been reported. We have measured for the first time the KER values for dissociation of CO^+ through the C + O^+ channel. Good agreement is found between our experimental results and theoretical reports [22–26].

This work was performed with financial support from CONACYT, CLAF and DGAPA-UNAM. The authors thank A. Bustos and A. Gonzalez for technical support.

References

1. S. Rosen, R. Peverall, M. Larsson, A. Le Padellec, J. Semaniak, A. Larson, C. Stromholm, J. Van der Zande, H. Danared, G.H. Dunn, Phys. Rev. A **57**, 4462 (1998)
2. K. Furuya, A. Matsuo, T. Ogawa, J. Phys. B: At. Mol. Opt. Phys. **35**, 3077 (2002)
3. C.M. Marian, M. Larsson, B.J. Olsson, P. Sigray, Chem. Phys. **130**, 361 (1989)
4. T. Masouka, E. Nakamura, Phys. Rev. A **48**, 4379 (1993)
5. K. Wang, V.J. Mckoy, Phys. Chem. **99**, 1643 (1995)
6. W. Kong, W. Hepburn, J. Chem. Phys. **99**, 1637 (1999)
7. M. Evans, C.Y. Ng, J. Chem. Phys. **111**, 8879 (1999)
8. Z. Bembenek, U. Domin, R. Kepa, K. Porada, M. Rytel, M. Zachwieja, Z. Jakubek, J.D. Janjic, J. Mol. Spectrosc. **165**, 205 (1994)
9. V.R. Bhardwaj, D. Mathur, K. Vijayalakshmi, P. Hvelplund, M.O. Larsson, C.P. Safvan, Phys. Rev. A **58**, 2834 (1998)
10. V. Sidis, J. Phys. Chem. **93**, 8128 (1989)
11. F.A. Gianturco, S. Kumar, Z. Phys. D **37**, 155 (1996)
12. W. Lu, P. Tosi, D. Bassi, J. Chem. Phys. **111**, 8852 (1999)
13. D. Dowek, D. Dhuicq, M. Barat, Phys. Rev. A **28**, 2838 (1983)
14. P. Lablanquie, J. Delwiche, M.-J. Hubin-Franskin, I. Nenner, P. Morin, K. Ito, J.H.D. Eland, J.-M. Robbe, G. Gandara, J. Fournier, P.G. Fournier, Phys. Rev. A **40**, 5673 (1989)
15. R.G. Cooks, J. Mass Spectrom. **30**, 1215 (1995)
16. C.E. Melton, G.F. Wells, J. Chem. Phys. **27**, 1132 (1957)
17. G. García, E. Mejía-Ospino, A. Guerrero, I. Álvarez, C. Cisneros, Int. J. Mass Spectrom. **261**, 53 (2007)
18. V. Krishnamurthi, K. Nagesha, V.R. Marathe, D. Mathur, Phys. Rev. A **44**, 5460 (1991)
19. A. Dantamaro, D.H. Katayama, J. Chem. Phys. **90**, 91 (1989)
20. T.F. Moran, J.B. Wilcox, L.E. Abbey, J. Chem. Phys. **68**, 261 (1978)
21. J. Lecointre, D.S. Belic, H. Cherkani-Hassani, J.J. Jureta, P. Defrance, J. Phys. B: At. Mol. Opt. Phys. **39**, 3275 (2006)
22. O.J. Orient, S.K. Srivastava, J. Phys. B: At. Mol. Opt. Phys. **20**, 3923 (1987)
23. N. Honjou, F. Sasaki, Mol. Phys. **37**, 1593 (1979)
24. M. Carlsson-Gothe, B. Wannberg, F. Falk, L. Karlsson, S. Svensson, P. Baltzer, Phys. Rev. A **44**, R17 (1991)
25. A.P. Hitchcock, P. Lablanquie, P. Morin, E. Lizon, A. Lugrin, M. Simon, P. Thiry, I. Nenner, Phys. Rev. A **37**, 2448 (1998)
26. J.B.A. Mitchell, H. Hus, J. Phys. B: At. Mol. Phys. **18**, 547 (1985)
27. A. Dadouch, G. Dujardin, L. Hellner, M.J. Besnard-Ramage, B.J. Olsson, Phys. Rev. A **43**, 6057 (1991)
28. K. Okada, S. Iwata, J. Chem. Phys. **112**, 1804 (2000)
29. F.B. Yousif, G. Hinojosa, J. de Urquijo, C. Cisneros, I. Alvarez, Int. J. Mass Spectrom. Ion Process. **171**, 127 (1997)
30. G. Hinojosa, F.B. Yousif, C. Cisneros, J. de Urquijo, I. Alvarez J. Phys. B: At. Mol. Opt. Phys. **32**, 915 (1999)
31. D.K. Gibson, J. Los, Physica **35**, 258 (1967)
32. D.K. Gibson, J. Los, J. Schopman, Physica **40**, 385 (1968)
33. S. Durup, P. Fournier, P. Döng, Int. J. Mass Spectrom. Ion Phys. **2**, 311 (1969)
34. S.J. Anderson, J. Chem. Phys. **60**, 3278 (1979)